# Asymptotically Dense Spherical Codes—Part II: Laminated Spherical Codes

Jon Hamkins, *Member, IEEE*, and Kenneth Zeger, *Senior Member, IEEE*

***Abstract*—New spherical codes called *laminated spherical codes* are constructed in dimensions $2$–$49$ using a technique similar to the construction of laminated lattices. Each spherical code is recursively constructed from existing spherical codes in one lower dimension. Laminated spherical codes outperform the best known spherical codes in the minimum distance sense for many code sizes. The density of a laminated spherical code approaches the density of the laminated lattice in one lower dimension, as the minimum distance approaches zero. In particular, the three-dimensional laminated spherical code is asymptotically optimal, in the sense that its density approaches the Fejes Tóth upper bound as the minimum distance approaches zero. Laminated spherical codes perform asymptotically as well as wrapped spherical codes in those dimensions where laminated lattices are optimal sphere packings.**

***Index Terms*—Asymptotic density, laminated lattices, packing, source and channel coding, spherical codes.**

## I. Introduction

### A. Overview

PART I of this two-paper series [1] described a technique to map any packing $\Lambda$ onto the unit $k$-dimensional sphere $S_k$. In the present paper (Part II), a new technique is introduced to construct spherical codes called laminated spherical codes. Whereas wrapped spherical codes were described by an explicit function that maps $\mathbb{R}^{k-1}$ onto the unit sphere $S_k$ for any $k \geq 2$, laminated spherical codes will be defined in a recursive manner using terminology and techniques from laminated lattice constructions. The laminated spherical codes improve upon previously known codes, and for low dimensions and many code sizes outperform the wrapped spherical codes described in [1]. Most of the known best spherical codes in three dimensions with less than about 30 000 codepoints and in four and five dimensions with less than about 150 codepoints are due to Hardin and Sloane [2]. For codes larger than the Hardin–Sloane codes, the laminated spherical codes introduced in this paper often give the best known performance.

See [1] for applications, definitions, and background of spherical codes. The basic notation and definitions in [1] will not be repeated here. Section I-B outlines some results and terminology regarding laminated lattices that will be useful in the remainder of the paper. Section II gives the formal construction of laminated spherical codes, derives their asymptotic density, and gives numerical comparisons.

Manuscript received December 11, 1995; revised June 8, 1997. This work was supported in part by the National Science Foundation, by Engineering Research Associates, Co., and by Joint Services Electronics Program. The material in this paper was presented in part at the IEEE International Symposium on Information Theory, Whistler, BC, Canada, September 1995.

J. Hamkins is with the Jet Propulsion Laboratory, Pasadena, CA 91109-8099 USA.

K. Zeger is with the Department of Electrical and Computer Engineering, University of California, San Diego, La Jolla, CA 92093-0407 USA.

Publisher Item Identifier S 0018-9448(97)07292-1.

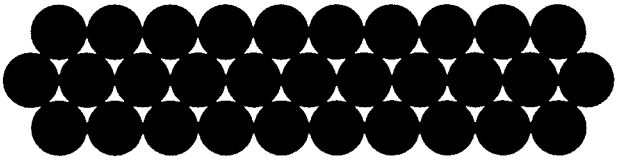

Fig. 1. The first three layers of $\Lambda_2$, which are stacked one on top of the other.

### B. Laminated Lattice Terminology

The notation and results in this section can be found in [3, ch. 6]. Given a set of points $P \subset \mathbb{R}^k$, a *nearest neighbor* to $X \in \mathbb{R}^k$ is a point of $P$ closest to $X$. A *Voronoi region* (or *Voronoi cell*), of a point $Z \in P$ is the set $\Pi$ of all points in $\mathbb{R}^k$ for which $Z$ is a nearest neighbor. If $f_P(X) = \inf_{Z \in P} ||X - Z||$, then a point $X \in \mathbb{R}^k$ is a *hole* if $f_P(X)$ is a local maximum and it is a *deep hole* if $f_P(X)$ is a global maximum. Note that the distance from a deep hole to the nearest point of $P$ is equal to the covering radius of $P$. Each vertex of a Voronoi cell has an associated *Delaunay cell*, which consists of the convex hull of the nearest neighbors of that point.

The one-dimensional laminated lattice is defined by

$$\Lambda_1 \equiv \mathbb{Z}.$$

The notation $\Lambda_k$ denotes the $k$-dimensional laminated lattice. Before giving the formal definition of $\Lambda_k$ for $k > 1$, an informal construction technique is discussed.

In two dimensions, $\Lambda_2$ is constructed by stacking copies of $\Lambda_1$, as shown in Fig. 1. In order to produce the densest lattice, the layers are stacked so that a lattice point of one layer is directly above a hole of the previous layer. Because $\Lambda_1$ is a lattice, if one lattice point in a layer is directly above a hole of the previous layer, then all lattice points of that layer are above holes of the previous layer. Note that the second, fourth, sixth, etc., layers above a given layer are translations of the given layer along the last coordinate only. Thus the layer number of $\Lambda_2$ is said to be two.

Similarly, $\Lambda_3$ is constructed by stacking up layers of $\Lambda_2$. The orientation of the lattice may be fixed so every point in a given layer has an identical last (third) coordinate. Again, the lattice points of one layer are placed opposite to (that is,

directly over, or differing in the last coordinate only) holes of the previous layer. In order to maintain the lattice property, namely, that the points of $\Lambda_3$ are closed under integer vector addition, the layer number of $\Lambda_3$ must be three. That is, the third, sixth, ninth, etc., layers are directly over the zeroth layer, i.e., a translation only in the last coordinate.

This procedure can be repeated indefinitely. In each new dimension, layers of $\Lambda_{k-1}$ are stacked as closely together as possible. More formally, for $k \geq 2$, a $k$-dimensional laminated lattice $\Lambda_k$ is a lattice whose minimum distance is one, whose sublattices include a $(k-1)$-dimensional laminated lattice, and whose density is the highest possible under these conditions. Thus $\Lambda_k$ can be decomposed as

$$\Lambda_k = \bigcup_{l=-\infty}^{\infty} \Lambda_{k-1}^{(l)}$$

where $\Lambda_{k-1}^{(l)}$ is the $l$th layer of $\Lambda_k$, i.e., a translation of $\Lambda_{k-1}$. Somewhat surprisingly, $\Lambda_k$ is not unique for all $k$, although the density of $\Lambda_k$ is unique. Since the layers are equinumerous, each point $X$ of one layer can be associated with a unique point $n(X)$ of the next layer. The point $n(X)$ is directly opposite a hole $h(X)$ of the layer containing $X$, i.e., $n(X)$ and $h(X)$ differ in the last coordinate only. That is, $h(X)$ has $n_{k-1}$ nearest neighbors in $\Lambda_{k-1}^{(l)}$, regardless of the choice of $X$ (one of these nearest neighbors is $X$). These nearest neighbor lattice points are denoted by $D(X)_1, \cdots, D(X)_{n_{k-1}}$, and the convex hull of these points forms a Delaunay cell. For any finite set of points $\mathcal{P} \subset \mathbb{R}^k$, define

$$H(\mathcal{P}) \equiv \underset{Y \in \mathcal{C}HULL(\mathcal{P})}{\operatorname{argmax}} \min_{X \in \mathcal{P}} \|X - Y\|$$

where it is understood that if there is no unique argument $Y$ which maximizes the expression above, any maximizing $Y$ may be chosen. $H(\mathcal{P})$ is a hole of $\mathcal{P}$ that lies within the convex hull of $\mathcal{P}$, and for each $X \in \mathcal{P}$

$$h(X) = H(\{D(X)_1, \cdots, D(X)_{n_{k-1}}\}).$$

We saw that for $\Lambda_2$ and $\Lambda_3$, the points of one component layer are opposite deep holes of adjacent layers. Since the covering radius $r$ of a layer is the distance from a deep hole to a lattice point, adjacent layers can be placed at a distance $\sqrt{1-r^2}$ from each other to maintain a minimum distance of one between all points. Unfortunately, it is not a simple matter to show from the definition of laminated lattices that layers are separated by $\sqrt{1-r^2}$ for higher dimensional laminated lattices. While this seems intuitively true, this question remains unproven for every $k > 12$, except $16, 24, 25, 26$, and $32$. As a result, the notion of subcovering radius is used. The *subcovering radius* $c_{k-1}$ of $\Lambda_{k-1}$ is defined such that $\sqrt{1-c_{k-1}^2}$ is the distance between layers of $\Lambda_k$. Note that $c_k$ is a lower bound on the covering radius of $\Lambda_k$. The values of $c_k$ are known for $k \leq 47$, and are tabulated in [3, p. 158] for laminated lattices that are scaled by a factor of two.

We define the *layer number* of $\Lambda_k$ as

$$l_k \equiv \min \left\{ i > 0 \colon \left(0, \cdots, 0, i\sqrt{1-c_{k-1}^2}\right) \in \Lambda_k \right\}. \quad (1)$$

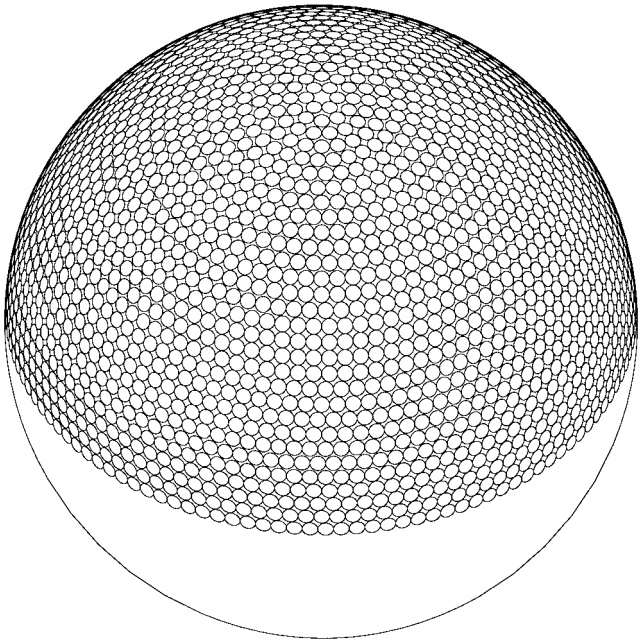

Fig. 2. The apple-peeling spherical code $\mathcal{C}_A(3,\ 0.05)$ has 4764 points.

The layer number is the smallest number of consecutive layers of $\Lambda_{k-1}$ stacked within $\Lambda_k$ such that the top layer is "directly over" the bottom layer, i.e., differing in the last coordinate only. For example, $l_2 = 2$, $l_3 = 3$, and $l_4 = 2$. Since adjacent layers of $\Lambda_k$ are separated by $\sqrt{1-c_{k-1}^2}$ and the distance between distinct points of $\Lambda_k$ is at least 1, it follows that $l_k\sqrt{1-c_{k-1}^2} \geq 1$.

## II. Laminated Spherical Codes

Laminated spherical codes of any size may be constructed, which provides a lower bound on achievable minimum distance as a function of code size. Our method is similar to those of [4] and [5] in that a projection from $k-1$ dimensions to $k$ dimensions is used; the difference lies in the placement of points prior to the projection. In Part I of this paper, we saw the apple-peeling code was not asymptotically optimal. In contrast, we shall show that the laminated spherical code density approaches the density of the laminated lattice $\Lambda_{k-1}$, as $d \to 0$, and thus the laminated spherical code is asymptotically optimal whenever $\Lambda_{k-1}$ is the densest $(k-1)$-dimensional packing.

Before presenting the formal construction technique, we describe informally how a three-dimensional laminated spherical code is constructed. To contrast the difference between the apple-peeling and laminated spherical codes, we show the apple-peeling code $\mathcal{C}(3, 0.05)$ in Fig. 2. The caps are arranged into shells (rings). Within each shell the caps are placed in an optimal two-dimensional scaled spherical (circle) code. That is, points are uniformly placed on the unit circle, and the circle is scaled and projected upward to $S_3$. This operation is done for each shell, and no effort is made to interlace caps of alternating shells.

In contrast, the laminated spherical code $\mathcal{C}_L(3, 0.05)$ is shown in Fig. 3. The caps are again placed in shells, but the caps of one shell interlace caps of the previous shell, thereby

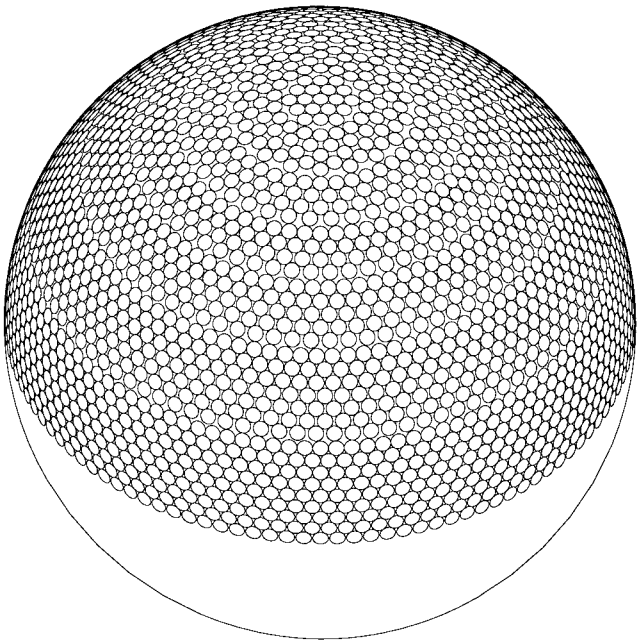

Fig. 3. The laminated spherical code $\mathcal{C}_L(3,\ 0.05)$ has 5244 points.

allowing the shells to be closer together. The interlacing is done in the same way as the stacking of layers in the construction of $\Lambda_2$. In the lattice construction $\Lambda_2$, a point of $\Lambda_2$ is placed directly over a hole of a previous layer in the lattice; analogously, a cap of $\mathcal{C}_L(3, 0.05)$ is placed in relation to a hole of a previous shell in the spherical code. Note that this procedure cannot be continued indefinitely on the sphere, as it leads to the spreading out of the caps as more shells are added.

To correct for this, the sphere is partitioned into annuli. The first shell in each annulus is packed very tightly—for general $k$, it is defined to be a scaled $(k-1)$-dimensional laminated spherical code that is projected onto $S_k$. For this example, this means it is a circle code, the same as a shell in the apple-peeling code. The remaining shells of the annulus are interlaced with their previous shell, and each of these has the same number of caps as the first shell. For minimum distances of 0.1 or less, the tighter packing of shells more than overcomes the spreading out of caps, and the laminated spherical code has more points than the apple-peeling code.

The laminated code in $\mathbb{R}^3$ may be viewed in two dimensions through the mapping $(x_1, \cdots, x_{k-1}, x_k) \to (x_1, \cdots, x_{k-1})$. The centers of the caps lie on concentric circles, each circle representing a shell, as shown in Fig. 4. The angle of a point on one of the circles is easy to compute, as it is the average of the angles of the two associated points of the previous shell. A formula for the radii of the shells is not as simple, but a radius is readily computed as the smallest number such that the caps of the given shell do not overlap the caps from the previous shell.

### A. Formal Construction of Laminated Spherical Codes

Let $k \le 49$ and $d \in (0, 1]$. For $k = 2$, a largest spherical code with minimum distance $d$ is obvious (although not unique); we denote such a code by $\mathcal{C}_L(2, d)$. For $k \ge 3$, we recursively define the $k$-dimensional *laminated spherical code* $\mathcal{C}_L(k, d)$ with minimum distance $d$ as follows:

$$\mathcal{C}_L(k, d) \equiv \left\{ \left( x_1, \cdots, x_{k-1}, \pm\sqrt{1 - \sum_{i=0}^{k-1} x_i^2} \right) : (x_1, \cdots, x_{k-1}) \in \bigcup_{i=0}^{N} r_i \mathcal{C}_i(k-1, d/r_{s(i)}) \right\} \tag{2}$$

where the radius of the $i$th shell is given at the bottom of this page. In the above, $s(i)$ is the index of the first shell of the annulus that contains the $i$th shell, defined by

$$s(i) \equiv g(\max\{j : r_{g(j)} \le r_i\})$$

where $g(i)$ is the index of the first shell of the $i$th annulus, given by

$$g(i) \equiv \min\{j : r_j > i d^{2/k}\}.$$

The total number of shells is given by

$$N \equiv \max\left\{ i : r_i \le \sqrt{1 - d^2/4} \right\}. \tag{3}$$

---

$$r_i \equiv \begin{cases} 0, & \text{if } i = 0 \\ d, & \text{if } i = 1 \\ r(i, 0), & \text{if } i > 1 \text{ and } \lfloor r_{i-1} d^{-2/k} \rfloor \ne \lfloor \max(r(i, 1), r(i - l_{k-1}, 0)) d^{-2/k} \rfloor \\ \max(r(i, 1), r(i - l_{k-1}, 0)), & \text{otherwise} \end{cases}$$

and where the tentative radii used above are defined by

$$r(i, b) \equiv \frac{r_{i-1}\left(1 - \frac{d^2}{2}\right)\sqrt{1 - b\left(\frac{c_{k-2} d}{r_{s(i-1)}}\right)^2} + d\sqrt{(1 - r_{i-1}^2)\left(1 - \frac{d^2}{4} - b\left(\frac{r_{i-1} c_{k-2}}{r_{s(i-1)}}\right)^2\right)}}{1 - b\left(\frac{r_{i-1} c_{k-2} d}{r_{s(i-1)}}\right)^2}.$$

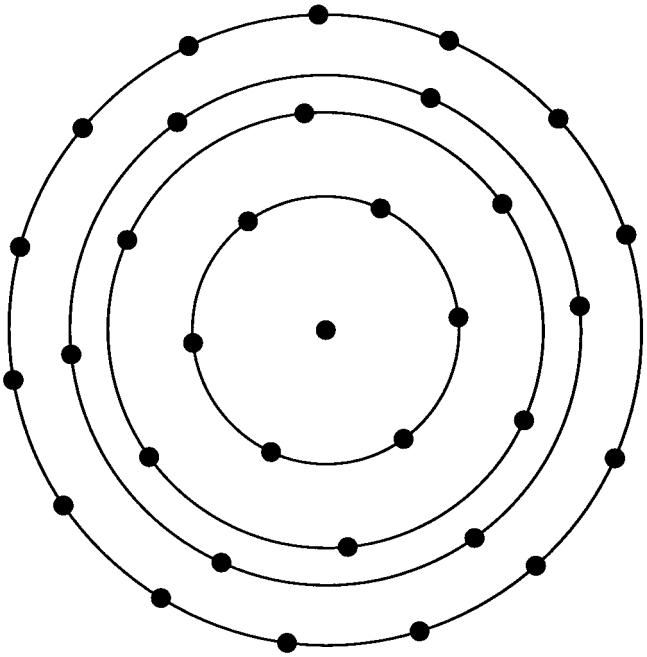

(a)

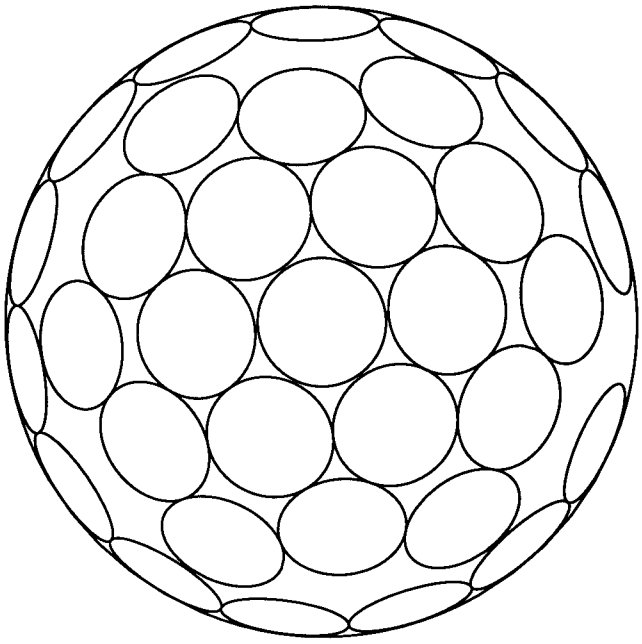

(b)

Fig. 4. (a) Five scaled two-dimensional codes. (b) Three-dimensional code derived from the two-dimensional codes by projecting codepoints out of the page, where codepoints are the centers of the caps.

The lower dimensional codes of (2) are given by

$$\mathcal{C}_{g(j)+l}(k-1,\, d) \equiv \begin{cases} \mathcal{C}_L(k-1,\, d), & \text{if } l=0 \\ f(\mathcal{C}_{g(j)+l-1}(k-1,\, d)), & \text{if } 1 \le l \le g(j+1)-g(j)-1 \end{cases}$$

i.e., it is either a $(k-1)$-dimensional laminated spherical code (if it is the first shell of an annulus) or a code that is interlaced with such a code (if it is a subsequent shell). We have used the function $f$ to define the holes of previous shells. The hole associated with $X$ may be defined by

$$f(X) \equiv \frac{H(L(X))}{||H(L(X))||}$$

where $L(X)$ is a set of points (from a previous shell) that correspond to a Delaunay cell of $\Lambda_{k-1}^{(l-1)}$, given by

$$L(X) \equiv \{w_{l-1}^{-1}(D(w_{l-1}(X))_i \colon 1 \le i \le n_{k-2}\}$$

where $w_l$ is

$$w_l(X) \equiv n(w_{l-1}(f^{-1}(X))).$$

*Remarks:*

- The sequence $\{r_i\}$ satisfies
$$0 = r_0 < \cdots < r_N \le \sqrt{1-d^2/4}.$$
- $\{r_i\}$ and $s(i)$ are defined in terms of each other, but each is well defined. In particular, $s(i-1)$ and $r_i$ each depend only on $r_0, \cdots, r_{i-1}$.
- $w_l(X)$: $\mathcal{C}_{g(j)+l}(k-1,\, d) \to \Lambda_{k-1}^{l}$ associates each point from a spherical code with a point on a laminated lattice.
- $L(X)$ associates
$$X \in \mathcal{C}_{g(j)+l}(k-1,\, d)$$
with a subset of $\mathcal{C}_{g(j)+l}(k-1,\, d)$ that is used to determine a point on the shell with radius $r_{g(j)+l+1}$.
- $l_k$ is defined in (1) and $c_k$, $D(\cdot)$, $H(\cdot)$, and $n(\cdot)$ are defined in Section I.

The following definitions are also used in the code construction:

$i$th shell:

$$r_i \mathcal{C}_i(k-1,\, d/r_{s(i)})$$

$i$th gap:

$$T_i \equiv \left\{ (x_1, \cdots, x_k) \in S_k \colon \sqrt{\sum_{i=1}^{k-1} x_i^2} \in (r_{i-1},\, r_i] \right\}$$

$i$th annulus:

$$A_i \equiv \bigcup_{j=g(i)+1}^{g(i+1)-1} T_j$$

$i$th buffer zone:

$$B_i \equiv \left\{ (x_1, \cdots, x_k) \in S_k \colon \sqrt{\sum_{i=1}^{k-1} x_i^2} \in (r_{g(i)-1},\, r_{g(i)}] \right\}$$

$$W_1 \equiv \left\{ (x_1, \cdots, x_k) \in S_k \colon \sqrt{\sum_{i=1}^{k-1} x_i^2} < d^{1/k} \right\}$$

$$W_2 \equiv \left\{ (x_1, \cdots, x_k) \in S_k \colon \sqrt{\sum_{i=1}^{k-1} x_i^2} > 1 - d^{1/k} \right\}$$

wasted regions:

$$W \equiv W_1 \cup W_2$$
$$T \equiv \bigcup_{i=0}^{\lceil d^{-2/k} \rceil - 1} A_i$$
$$B \equiv \bigcup_{i=1}^{\lceil d^{-2/k} \rceil - 1} B_i. \tag{4}$$

The $i$th *shell* is a $(k-1)$-dimensional spherical code scaled to a sphere of radius $r_i$. The points between the spheres of the $(i-1)$th and $i$th shells constitute the $i$th *gap*. We refer to the *$i$th annulus* as the set of points in $\mathbb{R}^{k-1}$ whose distance to the origin is in the interval $(r_{g(i)}, r_{g(i+1)-1}]$. That is, an annulus is a collection of consecutive gaps. Note that $s(i)$ is the smallest integer for which the set of all points whose magnitude is in the interval $(r_{s(i)}, r_i]$ lies in a single annulus. The *$i$th buffer zone* $B_i$ is the set of points lying between the $(i-1)$th annulus $A_{i-1}$ and $i$th annulus $A_i$. We call shells, gaps, annuli, and buffer zones which are projected onto the unit $k$-dimensional sphere $S_k$ again shells, gaps, annuli, and buffer zones, respectively. The sets $W_1$ and $W_2$ are referred to as *wasted regions*, in which codepoints are not necessarily as tightly packed as the rest of the sphere. The radii $\{r_i\}$ and the sets $W$, $T$, and $B$ are determined by the dimension of the spherical code $k$ and minimum distance $d$. For any $k$ and $d$, we have $S_k = W \cup T \cup B$, as seen in Fig. 5.

Each point in the spherical code $\mathcal{C}_L(k, d)$ corresponds to a unique point on the lattice $\Lambda_{k-1}$, since each point in the shell $\mathcal{C}_{g(j)+l-1}(k-1, d)$ corresponds to a unique point on the lattice $\Lambda_{k-2}^{l-1}$, via the function $w_{l-1}$. Recall that a lattice point $X \in \Lambda_{k-2}^{l-1}$ gives rise to the point $n(X) \in \Lambda_{k-2}^{l}$ via the hole $H(D(X)_1, \cdots, D(X)_{n_{k-1}})$. Likewise, a point $X \in \mathcal{C}_{g(j)+l-1}(k-1, d)$ gives rise to a point in $\mathcal{C}_{g(j)+l}(k-1, d)$ via the hole of the codepoints of $\mathcal{C}_{g(j)+l-1}(k-1, d)$ which correspond to $D(X)_1, \cdots, D(X)_{n_{k-1}}$, namely, $L(X)$. Thus $\mathcal{C}_{g(j)+l}(k-1, d)$ is equal to the set of (properly normalized) holes arising from $\mathcal{C}_{g(j)+l-1}(k-1, d)$, and $w_l$ is now also defined. For $k = 3$, the two-dimensional code layers can explicitly be written as

$$\mathcal{C}_{g(j)+i}(2, d) \equiv \begin{cases} \{(\cos(i\theta_{g(j)+i}), \sin(i\theta_{g(j)+i}))\}, & \text{if } i \text{ even} \\ \{(\cos((i+\frac{1}{2})\theta_{g(j)+i}), \sin((i+\frac{1}{2})\theta_{g(j)+i}))\}, & \text{if } i \text{ odd} \end{cases} \tag{5}$$

where $\theta_m \equiv 2\sin^{-1}(d/2r_{s(m)})$, $j \in \{0, \cdots, \lfloor 2\pi/\theta_i \rfloor - 1\}$, and $i \in \{0, \cdots, N\}$.

The laminated spherical code construction ensures that each $(k-1)$-dimensional code has minimum distance $d$. The sequence $\{r_i\}$ must be defined such that codepoints from different shells are at least distance $d$ from each other. This constraint is analogous to the separation of layers of $\Lambda_{k-2}$ in $\Lambda_{k-1}$, except that here we have the added complication that each layer (i.e., $(k-1)$-dimensional spherical code) is projected onto $S_k$.

The radius $r_i$ is recursively chosen as small as possible and yet large enough so that the points at radius $r_i$ are at least distance $d$ from the points at radius $r_{i-1}$, after the projection. Suppose $r_0, \cdots, r_{i-1}$ have been determined. Then $r_i$ is defined as the smallest positive number such that for each

$$X \equiv (x_1, \cdots, x_{k-1}) \in r_i \mathcal{C}_i(k-1, d/r_{s(i)})$$

and

$$Y \equiv (y_1, \cdots, y_{k-1}) \in r_{i-1} \mathcal{C}_{i-1}(k-1, d/r_{s(i)}),$$

the distance between the corresponding codepoints

$$X' = \left(x_1, \cdots x_{k-1}, \sqrt{1 - \sum_{i=1}^{k-1} x_i^2}\right)$$

and

$$Y' = \left(y_1, \cdots y_{k-1}, \sqrt{1 - \sum_{i=1}^{k-1} y_i^2}\right)$$

in $\mathcal{C}_L(k, d)$ is at least $d$ (see Fig. 6). That is, $r_i$ is chosen such that $||X' - Y'|| \geq d$.

Let $\delta$ be the distance from $Y$ to the hole associated with $Y$. Note that $\mathcal{C}_{i-1}(k-1, d/r_{s(i-1)})$ and $\mathcal{C}_{s(i)}(k-1, d/r_{s(i)})$ each have codepoints with angular separation $\theta_i$. Thus the distance from $Y$ to its associated hole is $r_{i-1}/r_{s(i-1)}$ times greater than

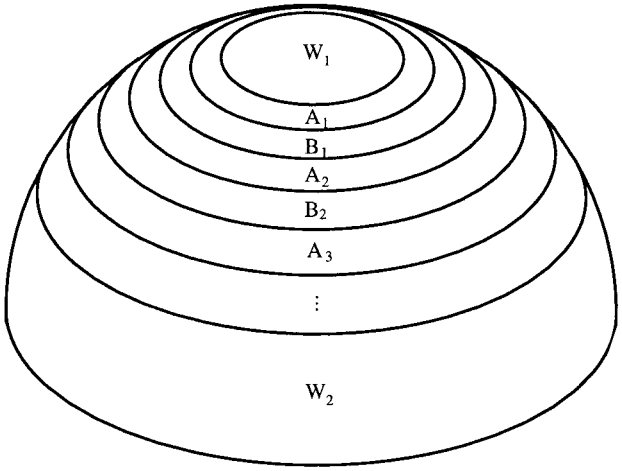


Fig. 5. The sphere (here $k = 3$) is partitioned into annuli, buffer zones, and wasted regions. In general, $W_1$ and $W_2$ may contain one or more annuli.

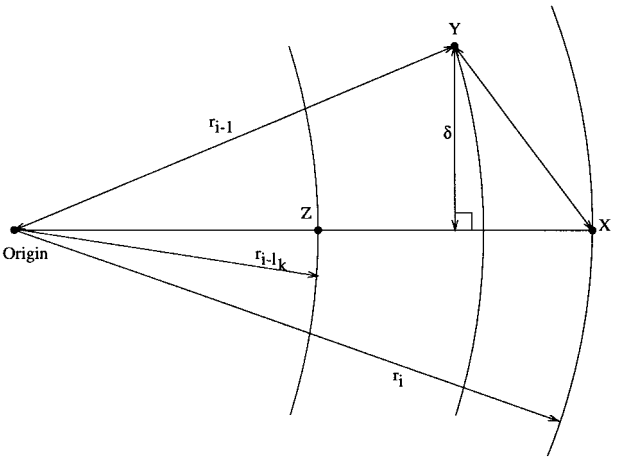


Fig. 6. Relation between $r_i$ and $r_{i-1}$.

the distance from a point in $\mathcal{C}_{s(i)}$ to its associated hole. Hence

$$\delta \geq \frac{r_{i-1}c_{k-2}d}{r_{s(i-1)}} \tag{6}$$

where the inequality comes from the fact that $c_{k-2}d$ is less than or equal to the distance from a point of $\mathcal{C}_{s(i)}(k-1, d)$ to its associated hole. Therefore, $r_i$ is chosen such that

$$d^2 \leq \|X'-Y'\|^2 \tag{7}$$

$$= \left(r_i - \sqrt{r_{i-1}^2-\delta^2}\right)^2 + \delta^2 + \left(\sqrt{1-r_{i-1}^2} - \sqrt{1-r_i^2}\right)^2. \tag{8}$$

Rearranging terms gives

$$\sqrt{(1-r_{i-1}^2)(1-r_i^2)} \leq 1 - d^2/2 - r_i\sqrt{r_{i-1}^2-\delta^2} \tag{9}$$

which upon squaring both sides and solving the quadratic for $r_i$ gives

$$r_i \geq \frac{\left(1-\frac{d^2}{2}\right)\sqrt{r_{i-1}^2-\delta^2} + \sqrt{(1-r_{i-1}^2)\left(d^2-\frac{d^4}{4}-\delta^2\right)}}{1-\delta^2}. \tag{10}$$

The negative solution for the quadratic equation is smaller than $r_{i-1}$ and is omitted. Taking the derivative of the right-hand side of (10) with respect to $\delta$ reveals that it is a decreasing function of $\delta$ when $\delta$ is the range for which (10) produces a real value. Thus using (6) and setting $r_i$ as in (11) (at the bottom of this page) ensures that $\|X'-Y'\| \geq d$.

The recursion for $r_i$ in (11) is used only when $Y$ belongs to the same annulus as $X$. If $r_{i-1}$ is the radius of the outermost shell in an annulus, then $r_i$ is defined such that every point on $r_iS_{k-1}$ is at least a distance $d$ from every point on the circle of radius $r_{i-1}$. This is equivalent to taking $\delta = 0$ in the solution above (i.e., when $\overrightarrow{YX}$ is directed radially outward), and gives

$$r_i = r_{i-1}\left(1-\frac{d^2}{2}\right) + d\sqrt{(1-r_{i-1}^2)\left(1-\frac{d^2}{4}\right)}. \tag{12}$$

While (11) ensures that the minimum distance between codepoints in a pair of adjacent shells is no more than $d$, it does not insure this condition for codepoints in nonadjacent shells. It is possible that (11) would result in codepoints from shell $i$ and shell $i+l_{k-1}$ which are closer than $d$. Let $X'$, $Y'$, and $Z'$, respectively, be the projections of $X$, $Y$, and $Z$ shown in Fig. 6, onto $S_k$. Then $Y'$, $X' \in \mathcal{C}_L(k, d)$. If $\|Z'-X'\| < d$, then (11) is not used, in which case $r_i$ is set to the value which produces $\|Z'-X'\| = d$ and from (12) gives

$$r_i = r_{i-l_{k-1}}\left(1-\frac{d^2}{2}\right) + d\sqrt{(1-r_{i-l_{k-1}}^2)\left(1-\frac{d^2}{4}\right)}. \tag{13}$$

In summary, the $r_i$'s may be determined by the algorithm at the bottom of this page.

### B. Example of a Laminated Spherical Code

We now illustrate the construction of a laminated spherical code for $k = 3$ and $d = 0.3$, using the formal definition. First, the radii $\{r_i\}$ are determined. Since in $\Lambda_2$ lattice points in one layer differ in the second coordinate from lattice points two layers away, we have $l_2 = 2$. In $\Lambda_1$, holes are a distance $1/2$ from two lattice points, and, hence, $c_1 = \frac{1}{2}$, and $n_1 = 2$. An iteration of the algorithm above gives $(r_0, \cdots, r_N) = (0, 0.3, 0.569, 0.752, 0.872, 0.978)$, $(s(0), \cdots, s(5)) = (0, 1, 2, 2, 2, 5)$, and $(g(0), \cdots, g(3)) =$

$$r_i = \frac{r_{i-1}\left(1-\frac{d^2}{2}\right)\sqrt{1-\left(\frac{c_{k-2}d}{r_{s(i-1)}}\right)^2} + d\sqrt{(1-r_{i-1}^2)\left(1-\frac{d^2}{4}-\left(\frac{r_{i-1}c_{k-2}}{r_{s(i-1)}}\right)^2\right)}}{1-\left(\frac{r_{i-1}c_{k-2}d}{r_{s(i-1)}}\right)^2} \tag{11}$$

```
r_0 := 0;
i := 1;
r_{s(i)} := r_1 := d;
while r_i ≤ √(1 − d²/4){
    i := i + 1;
    if ⌊r_{i−1} d^{−2/k}⌋ ≠ ⌊max(r(i, 1), r(i − l_{k−1}, 0)) d^{−2/k}⌋
        then r_{s(i)} := r_i := r(i, 0);                    /* begin new annulus */
    else r_i := max(r(i, 1), r(i − l_{k−1}, 0));            /* regular solution */
}
N := i − 1;
```

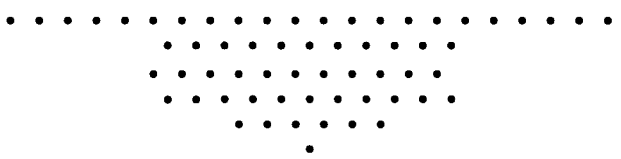

(a)

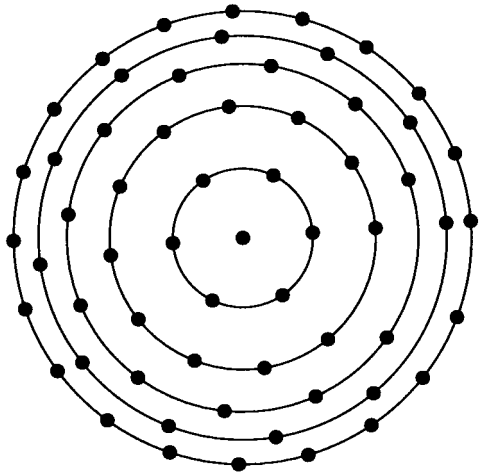

(b)

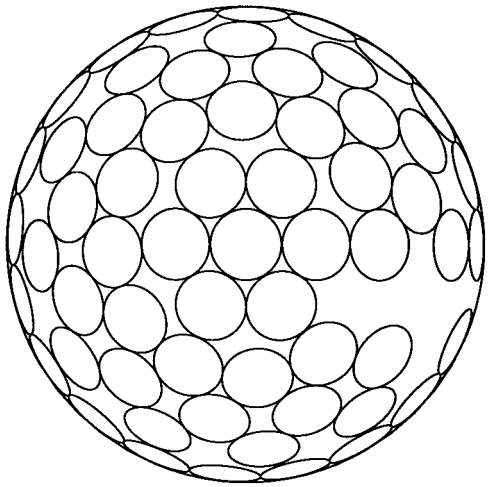

(c)

Fig. 7. A finite subset of $\Lambda_2$. (b) $\mathcal{C}_L(3, 0.3)$, before projection. (c) $\mathcal{C}_L(3, 0.3)$ after projection.

$(0, 1, 2, 5)$. Next, we determine the two-dimensional spherical codes to be projected onto $S_3$.

$i = 0$: $\mathcal{C}_i(k-1, d/r_{s(i)}) = \mathcal{C}_0(2, \infty) = \mathcal{C}_{g(0)+0}(2, \infty) = \mathcal{C}_L(2, \infty) = \{(1, 0)\}$.

$i = 1$: $\mathcal{C}_i(k-1, d/r_{s(i)}) = \mathcal{C}_{g(1)+0}(2, 1) = \mathcal{C}_L(2, 1) = \{(\cos(j\pi/3), \sin(j\pi/3)): 0 \le j \le 5\}$.

$i = 2$: $\mathcal{C}_i(k-1, d/r_{s(i)}) = \mathcal{C}_{g(2)+0}(2, 0.527)$. Thus $\theta_i = 2\sin^{-1}(0.527/2) = 0.533$, and $\mathcal{C}_i(k-1, d/r_{s(i)}) = \{(\cos(0.533j), \sin(0.533j)): 0 \le j \le 10\}$.

$i = 3$:

$$\begin{aligned}\mathcal{C}_i(k-1, d/r_{s(i)}) &= \mathcal{C}_{g(2)+1}(2, 0.527)\\ &= f(\mathcal{C}_i(2, 0.527))\\ &= \left\{\frac{H(L(X))}{\|H(L(X))\|}: \right.\\ &\qquad \left. X \in f(\mathcal{C}_i(2, 0.527))\right\}.\end{aligned}$$

If $Y \in \Lambda_1^0$, then $D(Y)_1 = Y$, $D(Y)_2 = Y + (1, 0)$, and so

$$\begin{aligned}n(Y) &= H(D(Y)_1, D(Y)_2) + \left(0, \sqrt{1 - c_{k-2}^2}\right)\\ &= Y + (1/2, \sqrt{3}/2).\end{aligned}$$

Let

$$X = (\cos(0.533j), \sin(0.533j)) \in \mathcal{C}_2(2, 0.527).$$

Then $w_0(X) \equiv (j, 0)$, and hence

$$\begin{aligned}L(X) &= \{w_0^{-1}(j, 0), w_0^{-1}(j+1, 0)\}\\ &= \{(\cos(0.533j), \sin(0.533j)),\\ &\qquad (\cos(0.533(j+1)), \sin(0.533(j+1)))\}.\end{aligned}$$

From this, we obtain,

$$\begin{aligned}&H(L(X))/\|H(L(X))\|\\ &\quad = (\cos(0.533(j+1/2)), \sin(0.533(j+1/2))).\end{aligned}$$

In the next shell, we use the fact that $w_1(X) = (j+1/2, \sqrt{3}/2)$. Letting $X$ range over $\mathcal{C}_2(2, 0.527)$ gives

$$\begin{aligned}&\mathcal{C}_i(k-1, d/r_{s(i)})\\ &\quad = \{(\cos(0.533(j+1/2)), \sin(0.533(j+1/2))):\\ &\qquad 0 \le j \le 10\}.\end{aligned}$$

$i = 4$:

$$\begin{aligned}\mathcal{C}_i(k-1, d/r_{s(i)}) &= \mathcal{C}_{g(2)+2}(2, 0.527)\\ &= \{(\cos(0.533j), \sin(0.533j)): 0 \le j \le 10\}.\end{aligned}$$

$i = 5$: A new annulus begins with $\mathcal{C}_{g(3)+0}(2, 0.307)$. Thus

$$\theta_i = 2\sin^{-1}(0.307/2) = 0.308$$

and

$$\begin{aligned}&\mathcal{C}_i(k-1, d/r_{s(i)})\\ &\quad = \{(\cos(0.308j), \sin(0.308j)): 0 \le j \le 19\}.\end{aligned}$$

The resulting code $\mathcal{C}_L(3, 0.3)$ is defined using (2) and has six shells. The shells contain 1, 6, 11, 11, 11, and 20 points,

TABLE I
THREE-DIMENSIONAL CODE SIZES AT VARIOUS MINIMUM DISTANCES

| $d$ | Coxeter upper bound | laminated code $\mathcal{C}_L$ | wrapped code $\mathcal{C}_W^{\Lambda_2}$ | apple-peeling code $\mathcal{C}_A$ |
|---|---|---|---|---|
| $10^{-1}$ | 1450 | 1294 | 1070 | 1236 |
| $10^{-2}$ | 145,103 | 134,422 | 130,682 | 125,504 |
| $10^{-3}$ | $1.45 \times 10^7$ | $1.43 \times 10^7$ | $1.40 \times 10^7$ | $1.26 \times 10^7$ |
| $10^{-4}$ | $1.45 \times 10^9$ | $1.45 \times 10^9$ | $1.44 \times 10^{9*}$ | $1.26 \times 10^9$ |
| $10^{-5}$ | $1.45 \times 10^{11}$ | $1.45 \times 10^{11}$ | $1.45 \times 10^{11*}$ | $1.26 \times 10^{11}$ |

* estimated

TABLE II
FOUR-DIMENSIONAL CODE SIZES AT VARIOUS MINIMUM DISTANCES. THE COXETER UPPER BOUND IS NOT ASYMPTOTICALLY TIGHT: USING THE BEST KNOWN UPPER BOUND ON PACKING DENSITY IN THREE DIMENSIONS AND OBSERVATION 1 OF [1], AN ASYMPTOTIC UPPER BOUND OF $2.79 \times 10^{3n+1}$ IS ACHIEVED, FOR $d = 10^{-n}$ AND LARGE $n$

| $d$ | Coxeter upper bound | laminated code $\mathcal{C}_L$ | wrapped code $\mathcal{C}_W^{\Lambda_3}$ | apple-peeling code $\mathcal{C}_A$ |
|---|---|---|---|---|
| $10^{-1}$ | 29,364 | 16,976 | 17,198 | 22,740 |
| $10^{-2}$ | $2.94 \times 10^7$ | $2.31 \times 10^7$ | $2.31 \times 10^{7*}$ | $2.28 \times 10^7$ |
| $10^{-3}$ | $2.94 \times 10^{10}$ | $2.59 \times 10^{10}$ | $2.59 \times 10^{10*}$ | $2.28 \times 10^{10}$ |
| $10^{-4}$ | $2.94 \times 10^{13}$ | $2.72 \times 10^{13}$ | $2.72 \times 10^{13*}$ | $2.28 \times 10^{13}$ |
| $10^{-5}$ | $2.94 \times 10^{16}$ | $2.77 \times 10^{16}$ | $2.77 \times 10^{16*}$ | $2.28 \times 10^{16}$ |

* estimated

respectively, and thus the entire code has 120 points. The unprojected two-dimensional codes are shown in Fig. 7(b). The spherical caps of the final code $\mathcal{C}_L(3, 0.3)$ are shown in Fig. 7(c). As $d$ approaches 0, the advantage of the laminating technique becomes more apparent. We compare the apple-peeling spherical code $\mathcal{C}^A(3, 0.05)$ to the laminated spherical code $\mathcal{C}_L(3, 0.05)$ in Fig. 8.

There are some improvements that may be made to the general construction. First, there may be points on the sphere that are not within distance $d$ of any codepoint, and thus these points may be added to the codebook. For example, on shells 3 and 4 of $\mathcal{C}_L(3, 0.3)$, it appears that an extra codepoint may be added without reducing the minimum distance. Also, we may modify the widths of the annuli, which would alter the number of shells that may be fit on the sphere, as well as their placement. The annulus width used above was $d^{2/k} \approx 0.448$. If the annulus width is set to zero instead, the apple-peeling code results. When the annulus width is 0.5, a code of size 128 may be obtained. In fact, each annulus width can be optimized separately.

### C. Asymptotic Density of the Laminated Spherical Code

Let $\Delta_{\mathcal{C}_L}(k, d)$ be the density of $\mathcal{C}_L(k, d)$, let

$$\Delta_{\mathcal{C}_L}(k) = \limsup_{d \to 0} \Delta_{\mathcal{C}_L}(k, d)$$

and let $\Delta_{\Lambda_k}$ be the density of the sphere packing with spheres of radius $1/2$ and centers in $\Lambda_k$. Within an annulus, layers of shells are stacked similarly to layers of lattices in a laminated lattice. Theorem 1 establishes that $\Delta_{\mathcal{C}_L}(k)$ is asymptotically equal to the density of the sphere packing generated by $\Lambda_{k-1}$.

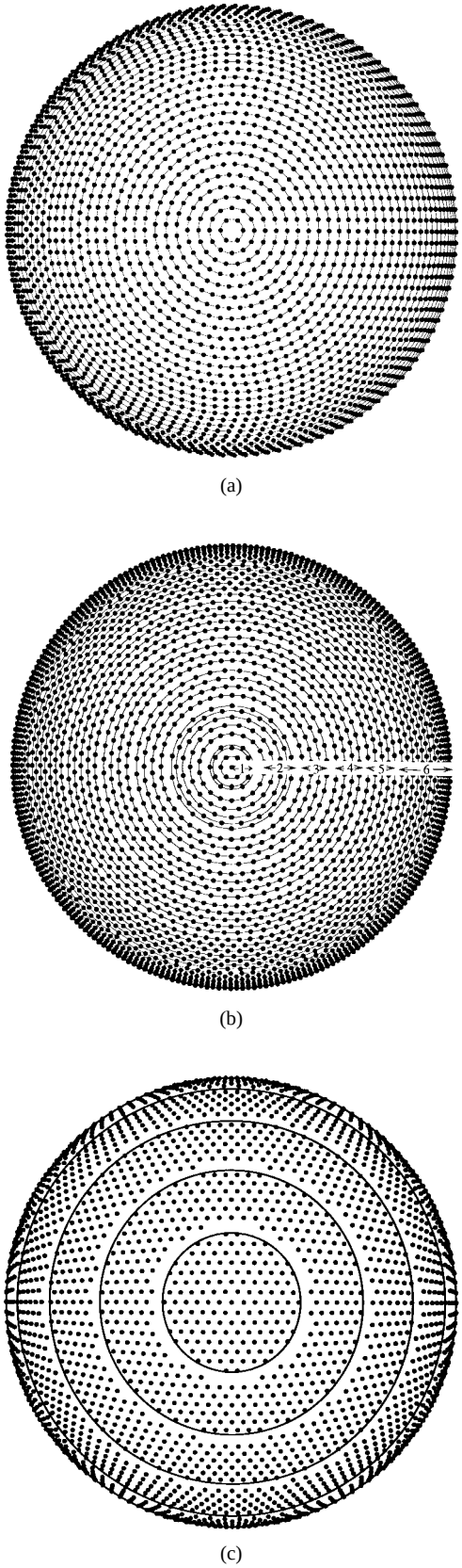


(a)

(b)

(c)

Fig. 8. Comparison of apple-peeling, laminated, and wrapped spherical codes. To obtain the spherical codes, the points shown in the circles are projected straight out of the page onto the surface of a sphere. (a) Apple-peeling code $\mathcal{C}_A(3, 0.05)$ has 4764 codepoints. (b) Laminated code $\mathcal{C}_L(3, 0.05)$ has 5244 codepoints. (c) Wrapped code $\mathcal{C}_W^{\Lambda_2}(3, 0.05)$ constructed from the hexagonal lattice has 4802 codepoints.

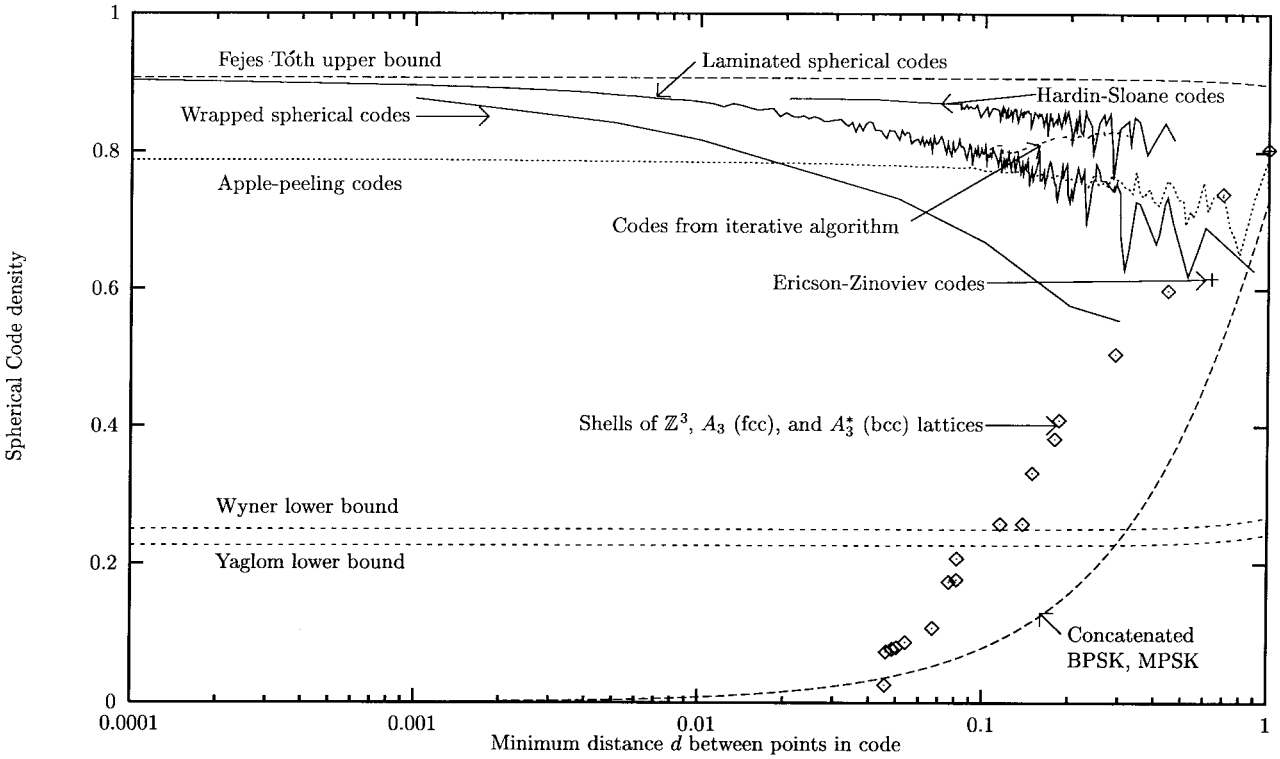


Fig. 9. Comparison of three-dimensional spherical codes.

*Theorem 1:* The density of a $k$-dimensional laminated spherical code $\mathcal{C}_L(k, d)$ with minimum distance $d$ is no more than $O(d^{1/k})$ less than the density of the $(k-1)$-dimensional laminated lattice $\Lambda_{k-1}$, for all $k \leq 49$. That is, $\Delta_{\mathcal{C}_L}(k, d) = \Delta_{\Lambda_{k-1}} - O(d^{1/k})$.

*Proof:* See the Appendix.

Corollary 1 follows from [1, Observation 1], Theorem 1, and the fact that $\Lambda_2$ is the densest possible packing in two dimensions. It also establishes the fact that the Fejes Tóth upper bound in [1, Observation 1] is asymptotically tight.

*Corollary 1:* The three-dimensional laminated spherical codes $\mathcal{C}_L(3, d)$ are asymptotically optimal as the minimum distance $d$ decreases to zero.

Fig. 9 shows the laminated spherical code density versus $d$. It includes unstructured codes found by a computer program of Hardin and Sloane [2]. This program has produced many of the best known codes. For some larger code sizes, we obtained codes using a simulating annealing approach which slightly improves upon [5]. This method produces good codes, but its computational complexity limits the code size that can be constructed. Spherical codes can also be generated from shells of lattices (e.g., [3], [6]). Fig. 9 shows the best codes in $\mathbb{R}^3$ generated among the first 1000 point-centered shells of the face-centered cubic and $Z_3$ lattices, whose minimum distances were obtained exactly. Fig. 9 also shows spherical codes formed from concatenations of $M$-ary Phase-Shift Keying (MPSK) and Binary Phase-Shift Keying (BPSK) codes. For $d < 0.7$, the laminated spherical code $\mathcal{C}_L(3, d)$ outperforms known codes derived from shells of lattices, and is comparable to the apple-peeling code. For $d < 0.02$, $\mathcal{C}_L(3, d)$ is the best code known, and convergence to the upper bound is apparent as $d \to 0$.

Fig, 10 shows density versus $d$, compared to other codes in $\mathbb{R}^4$. The qualitative performance is the same as for three dimensions, although the convergence of the density to its asymptotic value is slower. Still, for $d \leq 0.5$, the laminated spherical code outperforms spherical codes derived from shells of lattices $Z_4$, $A_4$, and $D_4$, or concatenated MPSK. Note that the Coxeter upper bound is not asymptotically tight, since the bound $\Delta_3^{\text{pack}} < 0.7784$ [7] is tighter.

Fig. 11 shows code size versus $d$, for various code constructions in $\mathbb{R}^8$. Here, the laminated spherical code $\mathcal{C}_L(8, d)$ is slower to converge towards the upper bound. The wrapped spherical code, presented in [1], outperforms most of the other codes for minimum distances less than about 0.4.

## III. Conclusions

A new technique was presented that constructs laminated spherical codes in dimensions up to 49. The three-dimensional laminated spherical codes are asymptotically optimal, in the sense that the ratio of the minimum distance of the constructed code to the upper bound given in [8] approaches one as the number of codepoints increases. This proves the upper bound is tight, asymptotically, and that previous lower bounds are not asymptotically optimal. The codes generated also compare favorably to other codes, for a wide variety of minimum distances. Good asymptotic performance is also achieved in higher dimensions, where the $k$-dimensional laminated spherical code density approaches the density of $\Lambda_{k-1}$. The question of whether asymptotic density of the $k$-dimensional laminated

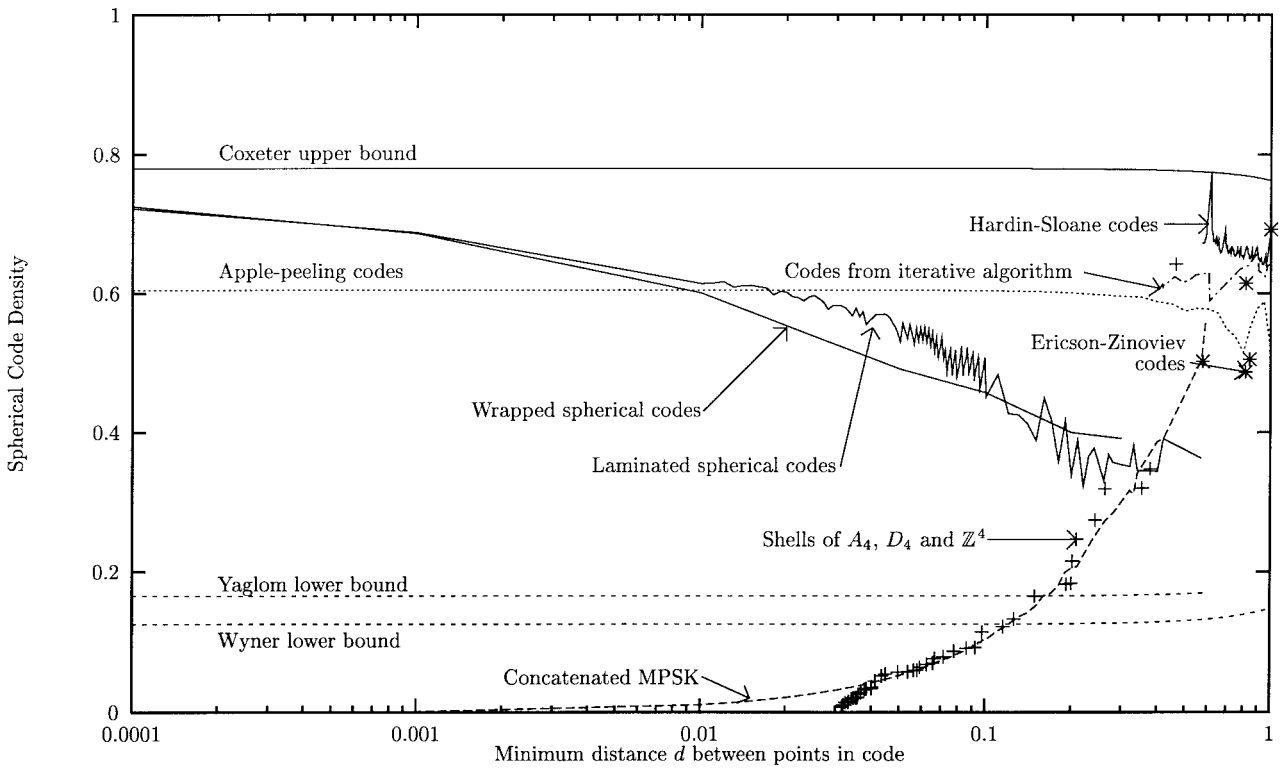


Fig. 10. Comparison of four-dimensional spherical codes.

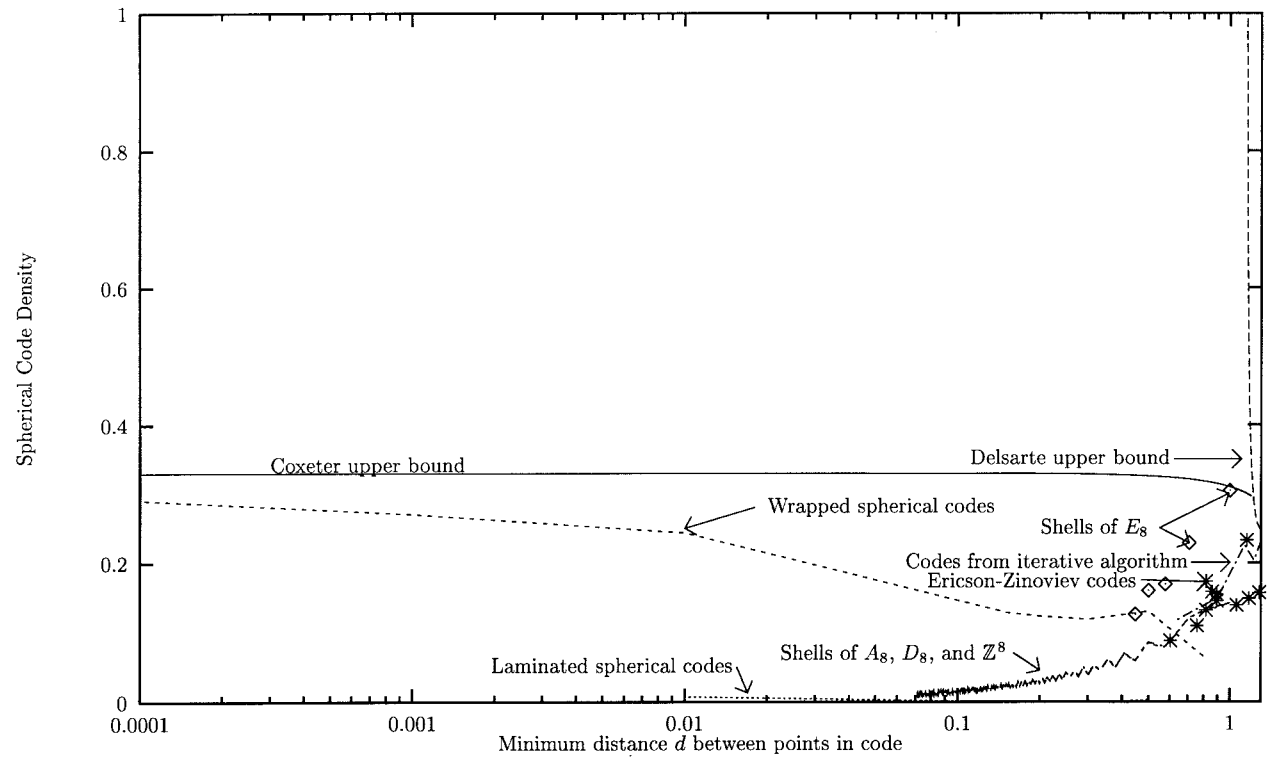


Fig. 11. Comparison of eight-dimensional spherical codes.

spherical code is optimal is equivalent to the question of whether the $\Lambda_{k-1}$ is the densest sphere packing.

Both wrapped spherical codes and laminated spherical codes presented in [1] improve upon the asymptotic performance of previous spherical codes. Similarly, the density of a wrapped spherical code with respect to a packing $\Lambda$ approaches the density of $\Lambda$, and hence, any densest lattice $\Lambda$ gives rise to an asymptotically optimal spherical code. The wrapped codes

are not restricted to laminated lattices; any lattice or packing in $\mathbb{R}^{k-1}$ may be used to construct a $k$-dimensional wrapped code.

The comparison of the nonasymptotic performance reveals that both the wrapped and laminated spherical codes perform better than other constructions, i.e., have larger code sizes for a given minimum distance. In three and four dimensions, the laminated spherical codes perform better than the wrapped codes. In higher dimensions, the advantages of wrapped spherical codes become more apparent: the wrapped codes are easier to construct than laminated spherical codes because an explicit mapping is specified instead of a recursive one, and the decoding algorithm reduces to a decoding algorithm for the underlying lattice, a well-studied problem.

For nonasymptotic spherical codes, an important question in channel decoding and quantization is how to find the nearest codepoint to an arbitrary point in $\mathbb{R}^k$. The laminated spherical codes can be decoded recursively in $O(\log |\mathcal{C}_L|)$ time. A detailed decoding algorithm can be found in [9].

## Appendix
## Proof of Theorem 1

Use induction on the dimension $k$. The claim holds for $k = 2$, since $\Delta_{\mathcal{C}_L}(2, d) > 1 - (d/2\pi)$ and $\Delta_{\Lambda_1} = 1$. Now suppose $k \geq 3$ and let

$$J \equiv \{i\colon d^{1/k} < r_i < 1 - d^{1/k}, \text{ where } r_i \text{ is determined by (11)}\}. \tag{14}$$

For each $i \in J$, the density $\Delta_{T_i}$ of gap $T_i$ of $\mathcal{C}_L$ shall be computed. The $(k-1)$-dimensional content (surface area) of $T_i$ is

$$A(T_i) = \int_{\sqrt{1-r_i^2}}^{\sqrt{1-r_{i-1}^2}} A_{k-1}(1-x^2)^{(k-3)/2}\,dx. \tag{15}$$

The integrand in (15) is monotonically nonincreasing in $x$, and hence

$$\left(\sqrt{1-r_{i-1}^2} - \sqrt{1-r_i^2}\right) r_{i-1}^{k-3} \leq \frac{A(T_i)}{A_{k-1}} \leq \left(\sqrt{1-r_{i-1}^2} - \sqrt{1-r_i^2}\right) r_i^{k-3}. \tag{16}$$

Using (11), we shall remove the occurrences of $r_i$ in (16). First, (11) will be put into an asymptotic form. In the following, constants encompassed by the $O$-notation do *not* depend on $i$. Since $r_i > d^{1/k}$ for all $i \in J$, $r_{s(i)} \geq d^{1/k} - d^{2/k} = \Omega(d^{1/k})$, and so

$$\left(1 - \frac{d^2}{2}\right)\sqrt{1 - \left(\frac{c_{k-2}}{r_{s(i)}}\right)^2} = \left(1 - \frac{d^2}{2}\right)\sqrt{1 - O(d^{2(1-(1/k))})} = 1 - O(d^{2(k-1)/k}). \tag{17}$$

Also,

$$\sqrt{1 - \frac{d^2}{4} - \frac{c_{k-2}^2 r_{i-1}^2}{r_{s(i)}^2}} = \sqrt{1 - \frac{c_{k-2}^2 r_{i-1}^2}{r_{s(i)}^2}} \cdot \sqrt{1 - \frac{d^2}{4\left(1 - \frac{c_{k-2}^2 r_{i-1}^2}{r_{s(+i)}^2}\right)}} \tag{18}$$

$$= \sqrt{1 - \frac{c_{k-2}^2 r_{i-1}^2}{r_{s(i)}^2}} - O(d^2) \tag{19}$$

where we have used the fact that

$$\frac{c_{k-2}^2 r_{i-1}^2}{r_{s(i)}^2} \leq c_{k-2}^2 \left[\frac{r_{s(i)} + d^{2/k}}{r_{s(i)}}\right]^2 \tag{20}$$

$$= c_{k-2}^2 [1 + O(d^{1/k})]^2 \tag{21}$$

$$= c_{k-2}^2 + O(d^{1/k}) \tag{22}$$

which is bounded away from 1 for sufficiently small $d$ because $c_{k-2}^2 \leq \frac{31}{32}$ for $k \leq 49$ [3]. Similarly,

$$\frac{r_{i-1}^2 d^2}{r_{s(i)}^2} = O(d^2(1 + d^{(2/k)-(1/k)})^2) = O(d^2) \tag{23}$$

and thus (11) can be rewritten as shown in (24)–(28) at the top of the following page. Hence, the left-hand and right-hand sides of (16) differ by $O(d^2)$. This gives

$$\frac{A(T_i)}{A_{k-1}} = \left(\sqrt{1-r_{i-1}^2} - \sqrt{1-r_i^2}\right) r_{i-1}^{k-3} + O(d^2) \tag{29}$$

$$= r_{i-1}^{k-2} d \sqrt{1 - \frac{c_{k-2}^2 r_{i-1}^2}{r_{s(i)}^2}} - O(d^{2(k-1)/k}) \tag{30}$$

$$\leq r_{i-1}^{k-2} d \sqrt{1 - c_{k-2}^2}, \tag{31}$$

where (31) holds for sufficiently small $d$. From [1, eq. (11)]

$$A(c(k, \theta/2)) = V_{k-1}(d/2)^{k-1}(1 - O(d^2)) \tag{32}$$

and thus the number of codepoints in each of shel $\mathcal{C}_{i-1}(k-1, d/r_{s(i)})$ and shell $\mathcal{C}_i(k-1, d/r_{s(i)})$ is

$$N_{s(i)} = \frac{\Delta_{\mathcal{C}_L}\left(k-1, \frac{d}{r_{s(i)}}\right) \cdot A_{k-1}}{A\left(c\left(k-1, \sin^{-1}\left(\frac{d}{2r_s(i)}\right)\right)\right)} \tag{33}$$

$$\geq \frac{\Delta_{\mathcal{C}_L}\left(k-1, \frac{d}{r_{s(i)}}\right) \cdot A_{k-1}}{V_{k-2}\left(\frac{d}{2r_s(i)}\right)^{k-2}} \tag{34}$$

$$= \frac{\Delta_{\mathcal{C}_L}(k-1, O(d^{(k-1)/k}))A_{k-1}}{V_{k-2}\left(\frac{d}{2r_s(i)}\right)^{k-2}} \tag{35}$$

where (34) holds for sufficiently small $d$, by (32). The density of spherical caps in $T_i$ is as shown in (36)–(40) on the following page, where (39) follows by induction on $k$. The density in (40) applies for all $i \in J$, i.e., all $i$ determined

$$r_i = \frac{r_{i-1}(1-O(d^{2(k-1)/k})) + d\sqrt{1-r_{i-1}^2}\left(\sqrt{1-\frac{c_{k-2}^2 r_{i-1}^2}{r_{s(i)}^2}} - O(d^2)\right)}{1-O(d^2)} \tag{24}$$

$$= r_{i-1} + d\sqrt{(1-r_{i-1}^2)\left(1-\frac{c_{k-2}^2 r_{i-1}^2}{r_{s(i)}^2}\right)} - O(d^{2(k-1)/k}) \tag{25}$$

and

$$\sqrt{1-r_i^2} = \left(1-\left(r_{i-1} + d\sqrt{(1-r_{i-1}^2)\left(1-\frac{c_{k-2}^2 r_{i-1}^2}{r_{s(i)}^2}\right)} - O(d^{2(k-1)/k})\right)^2\right)^{1/2} \tag{26}$$

$$= \sqrt{1-r_{i-1}^2}\left(1 - \frac{2r_{i-1}d\sqrt{1-\frac{c_{k-2}^2 r_{i-1}^2}{r_{s(i)}^2}}}{\sqrt{1-r_{i-1}^2}} + \frac{O(d^{2(k-1)/k})}{1-r_{i-1}^2}\right)^{1/2} \tag{27}$$

$$= \sqrt{1-r_{i-1}^2} - r_{i-1}d\sqrt{1-\frac{c_{k-2}^2 r_{i-1}^2}{r_{s(i)}}} + O(d^{2(k-1)/k}) \tag{28}$$

---

$$\Delta_{T_i} = \frac{N_{s(i)}A(c(k,\theta/2))}{A(T_i)} \tag{36}$$

$$\geq \frac{\left(\frac{\Delta_{\mathcal{C}_L}(k-1, O(d^{(k-1)/k}))\cdot A_{k-1}}{V_{k-2}\left(\frac{d}{2r_{s(i)}}\right)^{k-2}}\right)\cdot V_{k-1}(d/2)^{k-1}\cdot(1-O(d^2))}{A_{k-1}r_{i-1}^{k-2}d\sqrt{1-c_{k-2}^2}} \tag{37}$$

$$= \frac{\Delta_{\mathcal{C}_L}(k-1, O(d^{(k-1)/k}))V_{k-1}}{2V_{k-2}\sqrt{1-c_{k-2}^2}} - O(d^{1/k}) \tag{38}$$

$$= \frac{\Delta_{\Lambda_{k-2}}V_{k-1}}{2V_{k-2}\sqrt{1-c_{k-2}^2}}(1-O(d^{1/k})) - O(d^{1/k}) \tag{39}$$

$$= \frac{\Delta_{\Lambda_{k-2}}V_{k-1}}{2V_{k-2}\sqrt{1-c_{k-2}^2}} - O(d^{1/k}) \tag{40}$$

---

by (11) that are not in a wasted region. Now we repeat the argument for $r_i$ determined by (13). Let

$$J' \equiv \{i\colon d^{1/k} < r_i < 1-d^{1/k}, \text{ where } r_i \text{ is determined by (13)}\}. \tag{41}$$

If $J' \neq \phi$, let $i \in J'$ and let

$$R_i \equiv \bigcup_{j=i-l_{k-1}+1}^{i} T_j. \tag{42}$$

Then from (13)

$$r_i = r_{i-l_{k-1}} + d\sqrt{1-r_{i-l_{k-1}}^2} - O(d^2), \tag{43}$$

and

$$\sqrt{1-r_i^2} = \sqrt{1-r_{i-l_{k-1}}^2 - 2r_{i-l_{k-1}}d\sqrt{1-r_{i-l_{k-1}}^2} \pm O(d^2)} \tag{44}$$

$$= \sqrt{1-r_{i-l_{k-1}}^2}\left(1 - \frac{r_{i-l_{k-1}}d}{\sqrt{1-r_{i-l_{k-1}}^2}} \pm \frac{O(d^2)}{1-r_{i-l_{k-1}}^2}\right) \tag{45}$$

$$= \sqrt{1-r_{i-l_{k-1}}^2} - r_{i-l_{k-1}}d \pm O(d^{(2k-1)/k}). \tag{46}$$

$$\Delta_{R_i} = \frac{l_{k-1} N_{s(i)} A(c(k,\, \theta/2))}{A(R_i)} \tag{51}$$

$$\geq \frac{l_{k-1}\left(\dfrac{\Delta_{\mathcal{C}_L}(k-1,\, O(d^{(k-1)/k}))\cdot A_{k-1}}{V_{k-2}\left(\dfrac{d}{2r_{s(i)}}\right)^{k-2}}\right)\cdot V_{k-1}(d/2)^{k-1}\cdot(1-O(d^2))}{A_{k-1} r_{i-l_{k-1}}^{k-2} d(1\pm O(d^{1/k}))} \tag{52}$$

$$\geq \frac{\left(\dfrac{\Delta_{\mathcal{C}_L}(k-1,\, O(d^{(k-1)/k}))\cdot A_{k-1}}{V_{k-2}\left(\dfrac{d}{2r_{s(i)}}\right)^{k-2}}\right)\cdot V_{k-1}(d/2)^{k-1}\cdot(1\pm O(d^{1/k}))}{A_{k-1} r_{i-l_{k-1}}^{k-2} d\sqrt{1-c_{k-2}^2}} \tag{53}$$

$$\geq \frac{\Delta_{\Lambda_{k-2}} V_{k-1}}{2\sqrt{1-c_{k-2}^2}\, V_{k-2}} - O(d^{1/k}) \tag{54}$$

From (16), with $r_{i-1}$ replaced by $r_{i-l_{k-1}}$, we obtain

$$\left(\sqrt{1-r_{i-l_{k-1}}^2}-\sqrt{1-r_i^2}\right) r_{i-l_{k-1}}^{k-3} \leq \frac{A(R_i)}{A_{k-1}} \leq \left(\sqrt{1-r_{i-l_{k-1}}^2}-\sqrt{1-r_i^2}\right) r_i^{k-3}. \tag{47}$$

Again, the left-hand and right-hand sides differ by $O(d^2)$. Thus

$$\frac{A(R_i)}{A_{k-1}} = \left(\sqrt{1-r_{i-l_{k-1}}^2}-\sqrt{1-r_i^2}\right) r_{i-l_{k-1}}^{k-3} + O(d^2) \tag{48}$$

$$= r_{i-l_{k-1}}^{k-2} d \pm O(d^{(2k-1)/k}) \tag{49}$$

$$\leq r_{i-l_{k-1}}^{k-2} d(1\pm O(d^{1/k})). \tag{50}$$

The density of spherical caps in $R_i$ is as shown in (51)–(54) at the top of this page, where (53) follows from

$$l_{k-1} \geq 1/\sqrt{1-c_{k-2}^2}$$

and (54) follows from (37)–(40).

Since (40) and (54) are independent of $i$, the density of $T$ can be bounded as

$$\Delta_T \geq \frac{\Delta_{\Lambda_{k-2}} V_{k-1}}{2V_{k-2}\sqrt{1-c_{k-2}^2}} - O(d^{1/k}). \tag{55}$$

Since $r_j - r_{j-1} < d$, for all $j$, the $(k-1)$-dimensional content of any buffer zone is bounded above by $A_{k-1}d$. The number of buffer zones in this region is no more than $2\lceil d^{-2/k}\rceil$, where buffer zones with both positive and negative $k$th coordinates are included. Hence, the total $(k-1)$-dimensional content of $B = \cup_i B_i$ is bounded as

$$A(B) < 2A_{k-1} d\lceil d^{-2/k}\rceil = O(d^{(k-2)/k}) \tag{56}$$

and $A(W) = O(d^{1/k})$. Thus

$$\Delta_{\mathcal{C}_L}(k,\, d) \geq \frac{\Delta_T A(T)}{A_k} \tag{57}$$

$$= \Delta_T \frac{A_k - A(W) - A(B)}{A_k} \tag{58}$$

$$= \left(\frac{\Delta_{\Lambda_{k-2}} V_{k-1}}{2V_{k-2}\sqrt{1-c_{k-2}^2}} - O(d^{1/k})\right) \cdot \left(\frac{A_k - O(d^{1/k})}{A_k}\right) \tag{59}$$

$$= \frac{\Delta_{\Lambda_{k-2}} V_{k-1}}{2V_{k-2}\sqrt{1-c_{k-2}^2}} - O(d^{1/k}) \tag{60}$$

where (59) follows from (55). Since layers of $\Lambda_{k-1}$ within $\Lambda_k$ are separated by a distance of $\sqrt{1-c_{k-1}^2}$ and each lattice point is distance 1 from an adjacent point, we have

$$\Delta_{\Lambda_k} = \frac{\Delta_{\Lambda_{k-1}} V_k (\frac{1}{2})^k}{V_{k-1}(\frac{1}{2})^{k-1}\sqrt{1-c_{k-1}^2}} = \frac{\Delta_{\Lambda_{k-1}} V_k}{2V_{k-1}\sqrt{1-c_{k-1}^2}}. \tag{61}$$

Thus, $\Delta_{\mathcal{C}_L}(k,\, d) \geq \Delta_{\Lambda_{k-1}} - O(d^{1/k})$. □

## ACKNOWLEDGMENT

The authors wish to thank N. J. A. Sloane for pointing out some of the best spherical codes in three dimensions for codes up to 33 002 codepoints, and to A. Vardy for helpful discussions.

## REFERENCES

[1] J. Hamkins and K. Zeger, "Asymptotically dense spherical codes—Part I: Wrapped spherical codes," this issue, pp. 1774–1785.
[2] N. J. A. Sloane, anonymous ftp from netlib.att.com in directory netlib/att/math/sloane/doc, 1994.
[3] J. H. Conway and N. J. A. Sloane, *Sphere Packings, Lattices, and Groups.* New York: Springer-Verlag, 1993.
[4] I. M. Yaglom, "Some results concerning distributions in $n$-dimensional space," Appendix to Russian edition of Fejes Tóth, *Lagerungen in der Ebene, auf der Kugel und in Raum*, 1958.
[5] A. A. El Gamal, L. A. Hemachandra, I. Shperling, and V. K. Wei, "Using simulated annealing to design good codes," *IEEE Trans. Inform. Theory*, vol. IT-33, pp. 116–123, Jan. 1987.
[6] N. J. A. Sloane, "Tables of sphere packings and spherical codes," *IEEE Trans. Inform. Theory*, vol. IT-27, pp. 327–338, May 1981.
[7] J. H. Lindsey, II, "Sphere-packing in $R^3$," *Mathematika*, vol. 33, pp. 137–147, 1986.
[8] L. Fejes Tóth, "Kugelunterdeckungen und Kugelüberdeckungen in Räumen konstanter Krümmung," *Arch. Math.*, vol. 10, pp. 307–313, 1959.
[9] J. Hamkins, "Design and analysis of spherical codes," Ph.D. dissertation, Univ. of Illinois, Urbana-Champaign, IL, Sept. 1996.